


RESEARCH

Open Access



14-3-3 mitigates alpha-synuclein aggregation and toxicity in the in vivo preformed fibril model

Rachel Underwood^{1,3}, Mary Gannon¹, Aneesh Pathak¹, Navya Kapa¹, Sidhanth Chandra^{1,4}, Alyssa Klop¹ and Talene A. Yacoubian^{1,2*} 

Abstract

Alpha-synuclein (asyn) is the key component of proteinaceous aggregates termed Lewy Bodies that pathologically define a group of disorders known as synucleinopathies, including Parkinson's Disease (PD) and Dementia with Lewy Bodies. α syn is hypothesized to misfold and spread throughout the brain in a prion-like fashion. Transmission of asyn necessitates the release of misfolded asyn from one cell and the uptake of that asyn by another, in which it can template the misfolding of endogenous asyn upon cell internalization. 14-3-3 proteins are a family of highly expressed brain proteins that are neuroprotective in multiple PD models. We have previously shown that 14-3-3 θ acts as a chaperone to reduce asyn aggregation, cell-to-cell transmission, and neurotoxicity in the in vitro pre-formed fibril (PFF) model. In this study, we expanded our studies to test the impact of 14-3-3s on asyn toxicity in the in vivo asyn PFF model. We used both transgenic expression models and adenovirus associated virus (AAV)-mediated expression to examine whether 14-3-3 manipulation impacts behavioral deficits, asyn aggregation, and neuronal counts in the PFF model. 14-3-3 θ transgene overexpression in cortical and amygdala regions rescued social dominance deficits induced by PFFs at 6 months post injection, whereas 14-3-3 inhibition by transgene expression of the competitive 14-3-3 peptide inhibitor difopein in the cortex and amygdala accelerated social dominance deficits. The behavioral rescue by 14-3-3 θ overexpression was associated with delayed asyn aggregation induced by PFFs in these brain regions. Conversely, 14-3-3 inhibition by difopein in the cortex and amygdala accelerated asyn aggregation and reduction in NECA1-positive neuron counts induced by PFFs. 14-3-3 θ overexpression by AAV in the substantia nigra (SN) also delayed asyn aggregation in the SN and partially rescued PFF-induced reduction in tyrosine hydroxylase (TH)-positive dopaminergic cells in the SN. 14-3-3 inhibition in the SN accelerated nigral asyn aggregation and enhanced PFF-induced reduction in TH-positive dopaminergic cells. These data indicate a neuroprotective role for 14-3-3 θ against asyn toxicity in vivo.

Keywords: 14-3-3s, Alpha-synuclein, Parkinson's disease, Dementia with Lewy Bodies, Substantia nigra, Amygdala, Cortex, Mouse

Introduction

Alpha-synuclein (α syn) is a critical protein whose aggregation and transmission from cell to cell has been implicated in the neurodegenerative process in Parkinson's disease (PD) and Dementia with Lewy Bodies (DLB). α Syn is a highly expressed brain protein whose endogenous function is not well understood but likely includes

*Correspondence: tyacoubian@uabmc.edu

² Civitan International Research Center, Room 510A, 1719 Sixth Avenue South, Birmingham, AL 35294, USA

Full list of author information is available at the end of the article



© The Author(s) 2021. This article is licensed under a Creative Commons Attribution 4.0 International License, which permits use, sharing, adaptation, distribution and reproduction in any medium or format, as long as you give appropriate credit to the original author(s) and the source, provide a link to the Creative Commons licence, and indicate if changes were made. The images or other third party material in this article are included in the article's Creative Commons licence, unless indicated otherwise in a credit line to the material. If material is not included in the article's Creative Commons licence and your intended use is not permitted by statutory regulation or exceeds the permitted use, you will need to obtain permission directly from the copyright holder. To view a copy of this licence, visit <http://creativecommons.org/licenses/by/4.0/>. The Creative Commons Public Domain Dedication waiver (<http://creativecommons.org/publicdomain/zero/1.0/>) applies to the data made available in this article, unless otherwise stated in a credit line to the data.

regulation of synaptic transmission [1–3]. Thorough understanding of the mechanisms that regulate the aggregation, transmission, and toxicity of this protein could lead to new targets for therapeutic intervention in these disorders. We recently observed that the chaperone-like protein 14-3-3 θ is a critical regulator of the release, oligomerization, and toxicity of α syn in several cellular models [4]. 14-3-3 θ is a member of the highly homologous 14-3-3 protein family, which are multifunctional proteins that play a role in protein folding, protein trafficking, neurite growth, and cell survival among other cellular roles [5–11]. 14-3-3 θ is found to be colocalized with α syn in Lewy Bodies in both PD and DLB [12, 13]. We have observed a reduction in 14-3-3 θ expression in transgenic α syn mice and in soluble 14-3-3 levels in DLB brains [14–17]. Additionally, aberrant phosphorylation of 14-3-3 θ has been noted in both PD and DLB brains [15]. 14-3-3 θ overexpression protects against both neurotoxin and mutant LRRK2 toxicity, while 14-3-3 inhibition increases toxicity [6, 17–19].

Given 14-3-3s' roles in protein folding and trafficking, we recently examined the impact of 14-3-3s on α syn cell-to-cell transmission and toxicity in two separate cellular models: the paracrine α syn model and the in vitro α syn fibril model [4]. We found that 14-3-3 θ reduces α syn transfer and toxicity by inhibiting α syn oligomerization, seeding, and internalization, whereas 14-3-3 inhibition accelerates the α syn seeding and cell-to-cell transmission in these cellular models [4]. In the study described here, we expanded our work to examine the impact of 14-3-3 θ on α syn toxicity in vivo using the α syn preformed fibril (PFF) model. Here we describe the effect of 14-3-3 θ overexpression or 14-3-3 inhibition on behavioral deficits, α syn inclusion formation, and neuronal numbers in the PFF model. We observed that 14-3-3 θ overexpression reduced social dominance deficits, delayed α syn inclusion formation, and rescued reductions in tyrosine hydroxylase (TH)-positive neuronal counts, while pan 14-3-3 inhibition with the peptide inhibitor difopein accelerated behavioral deficits, α syn inclusion formation, and reductions in neuronal counts in the PFF model.

Material and methods

Mice

Mice were used in accordance with the guidelines of the National Institute of Health (NIH) and University of Alabama at Birmingham (UAB) Institutional Animal Care and Use Committee (IACUC). All animal work performed in this study was approved by UAB's IACUC. Transgenic mice expressing human 14-3-3 θ under the neuronal promoter Thy1.2 were previously developed by our group [4, 6]. Transgenic mice expressing difopein-enhanced yellow

fluorescent protein (eYFP) under the neuronal promoter Thy1.2 were obtained from Dr. Yi Zhou at Florida State University [20]. 14-3-3 θ hemizygous mice were crossed with C57BL/6 J mice from The Jackson Laboratory (catalog #000664; RRID: IMSR_JAX:000664) to produce 14-3-3 θ transgenic and wildtype littermate mice for stereotactic injections. Difopein hemizygous mice were also crossed separately with C57BL/6 J mice to produce difopein transgenic and wildtype littermate mice for stereotactic injections. C57BL/6 J mice from The Jackson Laboratory (catalog #000664; RRID: IMSR_JAX:000664) were purchased and homozygous bred to produce wildtype (WT) mice for AAV experiments.

Fibril preparation

Recombinant full-length mouse α syn protein was prepared as previously described and generously supplied by Dr. Laura Volpicelli-Daley and Dr. Andrew West [21, 22]. Before stereotactic injection in mice, fibrils were generated by incubating purified mouse monomeric α syn at a concentration of 5 mg/ml in 50 mM Tris (pH 7.4) with 166 mM KCl with constant agitation at 700 rpm at 37 °C for 7 days. Immediately prior to injection, α syn fibrils were sonicated with a water bath sonicator (QSonica, Newton CT) with 1 s sonication pulses separated by 1 s wait intervals, with every 15 s of sonication separated by 2 min for the total duration of 1 h at A = 30 at 4 °C. For verification of fibril quality, sonicated α syn fibrils were analyzed by dynamic light scattering (DLS) on a DynaPro NanoStar (Wyatt Technology, Santa Barbara CA) every morning of injection to ensure sonicated fibril average radius was between 20–50 nm prior to injection (Additional file 1: Figure S1). A subset of unsonicated and sonicated fibrils were examined by transmission electron microscopy (TEM) to confirm fibrillar size and morphology (Additional file 1: Figure S1).

AAV preparation and injection

AAV2/CBA-IRES2-eGFP-WPRE (AAV-GFP) and AAV2/CBA-14-3-3 θ -V5-his-IRES-eGFP-WPRE (AAV-14-3-3 θ) were constructed as previously described [18, 23]. Equal numbers of male and female C57BL/6 mice from Jackson Laboratories were deeply anesthetized with 5% isoflurane and maintained at 0.25%–4% during surgery for stereotactic injection at 8 weeks with AAV into the SN [anteroposterior (AP): –3.0 from bregma; mediolateral (ML): –1.3 from midline; dorsoventral (DV): –4.6 below dura]. Mice were injected with 2 μ l of either AAV-GFP (titer: 1.8E + 12 vg/ml, viral genomes/ml) or AAV-14-3-3 θ (titer: 7.0E + 11 vg/ml) at a rate of 0.25 μ l/min using a microinjection pump.

Stereotactic injections of PFFs

Equal numbers of male and female mice at 8–12 weeks of age were deeply anesthetized with 5% isoflurane and maintained at 0.25–4% during surgery for PFF injection. WT mice injected with AAV-GFP or AAV-14-3-30/GFP at 8 weeks of age were then injected at 12 weeks of age with PFFs. 14-3-30, difopein, or WT littermates were injected at 8–12 weeks of age with PFFs. Mice were unilaterally injected with 5 μ g of α syn fibrils or monomer (2 μ l of 2.5 mg/ml) at a flow rate of 0.250 μ l/minute into the dorsolateral striatum (AP: 0.2 mm from bregma; ML: –2 mm from midline; DV: –2.6 mm below dura), according to a previously established protocol [24]. Post-surgery mice were allowed a minimum of 15 min recovery time on a heating pad. All mice were observed until fully awake and non-drowsy to ensure successful recovery. Mice were given buprenorphine (1 mg/kg) 20 min prior to surgery and the day after to minimize pain and discomfort.

Immunohistochemistry

Mice were perfused with PBS followed by 4% paraformaldehyde using a forced pump system. After dissection, brains were sliced by microtome in 40 μ m thick coronal sections. Every sixth section from the anterior brain (including the sensorimotor and striatal regions) was stained for pS129 α syn or NECAB1 immunohistochemistry, while every fourth section from the posterior sections (including the SN) was stained for pS129 α syn or TH immunohistochemistry. For pS129 α syn and TH immunohistochemistry, sections were quenched with 0.6% hydrogen peroxide in methanol followed by antigen retrieval (10 mM sodium citrate, 0.05% Tween-20, pH 6.0) for 1 h at 37° C. Sections were then blocked in 5% normal goat serum (NGS) with 0.3% Triton X-100 and incubated for 48 h in pS129- α syn antibody (Abcam #51253) or 24 h in TH antibody (Pelfreez #40101) in 1.5% NGS at 4 °C. After washing, sections were incubated with goat anti-rabbit IgG biotinylated secondary antibody (Vector Laboratories #BA-1000) for 4 h at 4 °C. After washing with TBS, sections were incubated in ABC solution (Vector) for 30 min and developed using ImmPACT DAB Chromagen Solution (Vector). Following washing with TBS, sections were mounted on slides and progressively dehydrated with ethanol and Histo-clear. Slides were cover-slipped with Permount (Avantar) and imaged using an Olympus BX51 epifluorescence microscope. For pS129- α syn positive inclusion counts, 3 sections in either the sensorimotor cortical regions (Bregma +1.54 mm to +0.62 mm) or the SN (Bregma –2.70 mm to –3.88 mm) per well were selected and quantitated using ImageJ with the rater blind to experimental conditions.

One section was selected in the central and basolateral amygdala region (Bregma –0.82 mm to –1.34 mm) and quantitated using ImageJ with the rater blind to experimental conditions. α Syn inclusion counts were normalized per mm² area.

For fluorescence staining, sections were washed in TBS followed by antigen retrieval (10 mM sodium citrate, 0.05% Tween-20, pH 6.0) for 1 h at 37 °C. Sections were then blocked in 5% NGS with 0.1% Triton X-100 and incubated with anti-NECAB1 rabbit antibody (Sigma Millipore #HPA023629), anti-NeuN mouse antibody (ThermoFisher Scientific #14H6L24 or Sigma Millipore #MAB377), anti-GFAP mouse antibody (Sigma Millipore, #MAB360), or pS129- α syn rabbit antibody (Abcam #51253) overnight at 4 °C. After washing with TBS, sections were incubated with Cy3-conjugated goat anti-mouse secondary antibody and Alexa488-conjugated goat anti-rabbit antibody for 2 h at 4 °C. Sections were mounted on slides, cover-slipped using ProLong Diamond Antifade mounting solution (ThermoFisher Scientific), and imaged using an Olympus BX51 epifluorescence microscope or a Nikon Eclipse Ti2 confocal microscope. For NECAB1-positive neuronal counts, 3 sections in the sensorimotor cortical regions (Bregma +1.54 mm to +0.62 mm) per well were selected and quantitated using ImageJ with the rater blind to experimental conditions. NECAB1 counts were normalized to mm² area.

Stereology

Stereological estimates of TH-positive neuronal numbers were performed using the optical fractionator method of the StereoInvestigator 8.0 software from MBF Biosciences (MicroBrightfield Inc., Williston, VT, USA), as previously described [18, 25]. For each animal, SNpc regions of every fourth section based on systematic random sampling were outlined according to published mouse atlas (Bregma –2.70 mm to –3.88 mm). A grid was placed randomly over the outlined region for counting. At each counting frame (50 μ m \times 50 μ m) of the grid predetermined by the software setup, neurons with visible nuclei were counted within three-dimensional optical dissectors set to 20 μ m with a 60 \times oil immersion objective using an Olympus BX51 Microscope. A 1- μ m guard distance from the top and bottom of the section surface was excluded from each dissector. Section thickness was measured at every tenth counting frame on each section to obtain the actual thickness after tissue processing. The total number of neurons (N_{total}) was calculated using the equation: $N_{total} = N_{counted} \times 1/ssf \times 1/asf \times 1/hsf$, where $N_{counted}$ is the number of neurons counted, ssf is the section sampling fraction, asf is the area sampling fraction and hsf is the height sampling fraction.

Coefficient of error (Gundersen, $m=1$) was set to <0.1 . Stereology estimates were done with the investigator blinded to the experimental condition.

Behavior tests

Behavior tests to assess motor and social functions were conducted 3 and 6 months after PFF injection. Mice were handled for 3 to 5 days before testing began and habituated to testing room for 30 min at the start of each testing day. Behavior tests began at least 1 h after light/dark cycle switch and completed at least 1 h before switching back to their dark cycle. In order to minimize stress to the animals, behavior tests were ordered from least to most stressful as follows: open field, wire hang, social dominance (tube test), pole test, and finally rotarod. Behavior was done primarily at 6 months post injection (mpi), but the difopein cortical cohort did undergo behavioral tests at 3 mpi. All behavior apparatuses were cleaned with 2% chlorohexidine between trials in order to minimize scent contamination between mice. Further, male mice were tested before female mice to minimize their exposure to female scent.

Open field

For open field, mice were placed with a 48 in. \times 48 in. open arena with clear plexi-glass walls. Mice were videoed for 4 min using EthoVision software and analyzed for overall velocity, distance moved across all planes (vertical and horizontal), and time spent in the periphery.

Wire hang

A four limb wire hang test was performed, as previously described with some modifications [26]. An apparatus with a wire grid bottom and angled edges to prevent mice from crawling over was built by the UAB machine shop. This apparatus was attached to a ring stand approximately 1 m high over a rat cage filled with bedding. The apparatus was inverted and a mouse was set on top. The apparatus was then flipped back over, so that the mouse was upside down and had to hang onto the wire grid in order to stay on. If the mouse was still hanging on after 60 s, it was removed and placed back in its home cage. A total of 2 trials per mouse were run, and all the mice in the cohort were run on the first trial before beginning the second trials, giving an interval of about 90 min between the two trials.

Tube test

For the tube test, mice were placed in a clear 12" long tube at opposing ends as previously described in protocols established by Arrant et al. [27, 28]. Mice were not released until both mice had all four paws inside the tube. Male mice were tested in a 1½" diameter tube, and

females were tested in a 1" diameter tube to account for differences in size between sexes. Each PFF-injected WT mouse, monomer-injected transgenic 14-3-3 θ or difopein mouse, and PFF-injected transgenic 14-3-3 θ or difopein mouse was randomly matched against 3 different monomer-injected WT mice of the same age and gender in separate trials. The PFF-injected WT mouse, monomer-injected transgenic 14-3-3 θ or difopein mouse, and PFF-injected transgenic 14-3-3 θ or difopein mouse were given 2 min to habituate in the testing arena before introduction of the monomer-injected WT mouse. Mice were given a 2-min rest between rounds and tested over a 2 day period.

Pole test

At 3 mpi (aged 5–6 months), mice were placed facing upwards at the top of a ¼" diameter round 3-foot long pole. Each mouse was timed for the duration to turn downwards down the pole as well as descend to the bottom of the pole. At 6 mpi (mouse age 8–9 months), wire footholds were added to the pole to assist mice in descending safely due to age and weight gain.

Rotarod

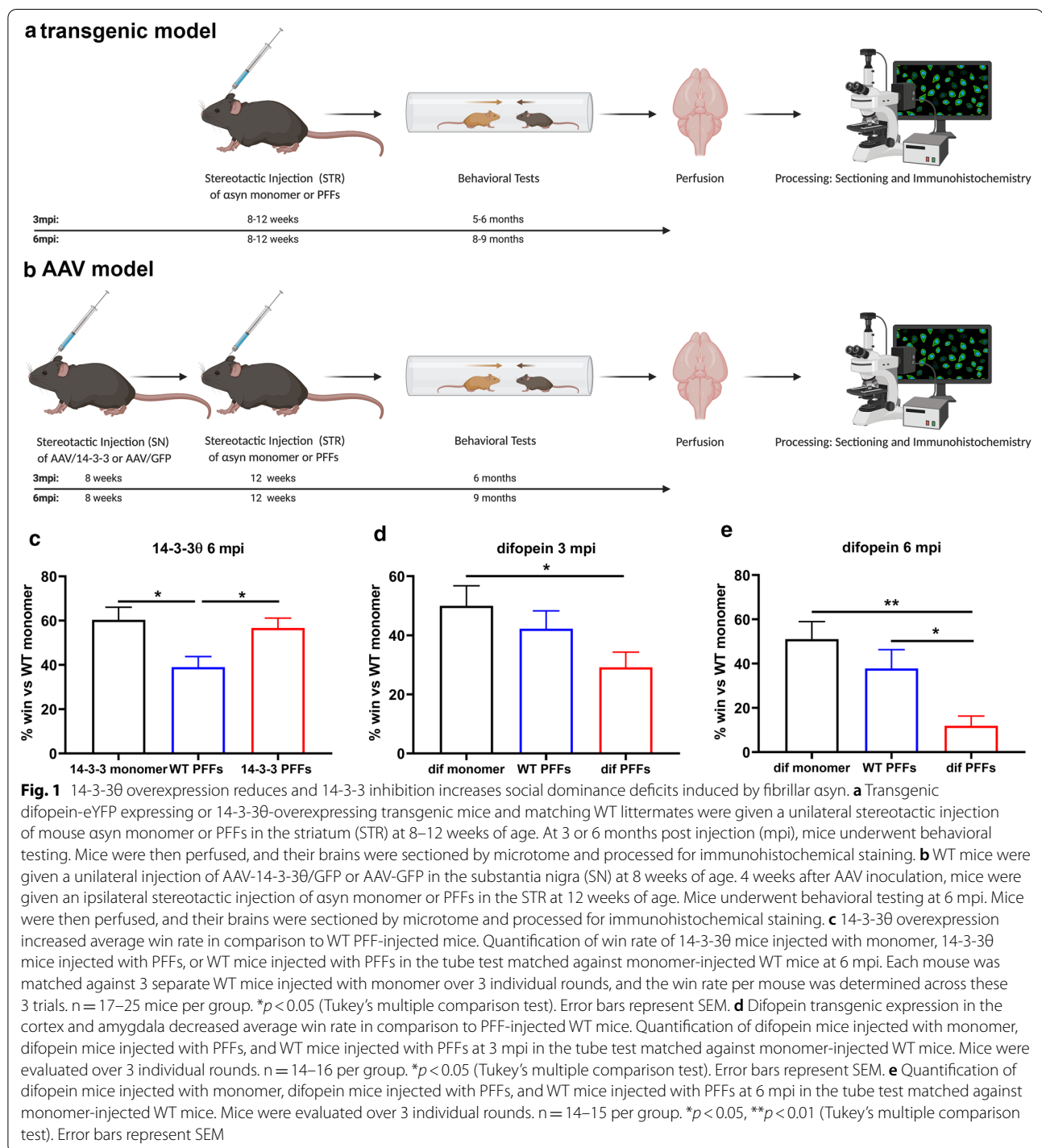
To further assess motor activity at 6 mpi, mice were placed on an accelerating rotarod apparatus with speed increasing from 5 to 35 rpm over 60 s. Mice were given 3 days of training on the apparatus and 2 days of testing. All mice underwent 3 trials per day with an inter-trial rest time of 2 min on training days and 5 min on assessment days. No mice failed to fall during the allotted 60 s.

Statistical analysis

GraphPad Prism 8 (La Jolla, CA) was used for statistical analysis of experiments. Data were analyzed by either Student's *t*-test, one-way ANOVA, or two-way ANOVA, followed by post-hoc pairwise comparisons using Tukey's multiple comparison tests. Statistical significance was set at $p \leq 0.05$. All the details of experiments can be found in the results section or figure legends. All data values are presented as mean \pm SEM. ANOVA related statistics (*F* statistic, *p* values) are noted in the results section, while the post-hoc test results are found in the figure legends. For *t*-tests, the *t* statistic and *p* values are noted in the results section.

Results

To test the impact of 14-3-3 proteins on *asyn* pathogenesis in vivo, we examined the effect of 14-3-3 θ overexpression or 14-3-3 inhibition on behavioral deficits, *asyn* inclusion formation, and neuronal counts in the in vivo fibril model (Fig. 1a, b). We previously created a transgenic mouse that overexpresses 14-3-3 θ tagged with the



HA tag under the Thy1.2 promoter [4, 6]. This transgenic mouse expresses HA-tagged 14-3-3θ in neurons located in the cortex, hippocampus, amygdala, and other areas, but no HA-tagged 14-3-3θ is detected in dopaminergic neurons in the SN (Additional file 2: Figure S3b). This mouse was used to examine the impact of 14-3-3θ

manipulation in the cortex and amygdala (Fig. 1a). We also examined the impact of 14-3-3θ overexpression in the SN by using an adeno-associated virus (AAV) expressing 14-3-3θ-GFP that was injected into the SN by stereotactic means (Fig. 1b). For testing the impact of 14-3-3 inhibition with the pan-14-3-3 peptide inhibitor

difopein, we used 2 different lines expressing difopein-eYFP under the Thy1.2 promoter [20]: (1) line 132, which primarily expresses difopein-eYFP in neurons in the cortex and amygdala but not within the SN, and (2) line 166, which expresses difopein-eYFP in TH-positive neurons in the SN but does not have expression in the cortex (Fig. 4a, d; Additional file 3: Figure S4a).

14-3-3 θ overexpression reduces social dominance behavioral deficits induced by α syn fibrils

Previous studies have shown motor and/or cognitive behavioral effects in response to α syn PFF injection into the dorsolateral striatum [24, 28, 29]. WT and 14-3-3 θ transgenic littermates were injected unilaterally with monomeric or fibrillary α syn (5 μ g) into the dorsolateral striatum at 8 to 12 weeks of age. Six months after PFF injection, we examined motor and non-motor behaviors in these mice. In the open field test, we observed no difference in velocity (2-way ANOVA: genotype F (1, 45) = 0.2994, p = 0.5870; PFF treatment F (1, 45) = 1.079, p = 0.3044; interaction F (1, 45) = 0.008179, p = 0.9283) or distance traveled (2-way ANOVA: genotype F (1, 45) = 0.2940, p = 0.5903; PFF treatment F (1, 45) = 1.088, p = 0.3024; interaction F (1, 45) = 0.007373, p = 0.9320) between WT and 14-3-3 θ transgenic mice, whether injected with monomeric or fibrillar α syn (Additional file 4: Figure S2a, b). We did observe an increase in the time 14-3-3 θ mice spent in the periphery of the open field arena compared to WT mice, which may suggest an increase in anxiety with 14-3-3 θ overexpression; however, PFF injection did not impact time spent in the periphery (2-way ANOVA: genotype F (1, 45) = 9.556, p = 0.0034; PFF treatment F (1, 45) = 0.5662, p = 0.4557; interaction F (1, 45) = 0.6048, p = 0.4408; Additional file 4: Figure S2c). While some studies have shown a motor deficit in mice injected with PFFs at 6 mpi on the pole test or rotarod test [24], we did not observe a consistent deficit in WT animals injected with PFFs on either test at 6 mpi (Additional file 4: Figure S2d, e). We also did not observe any differences in monomeric or fibrillar α syn-injected 14-3-3 θ mice with regard to motor function on the pole test (2-way ANOVA: genotype F (1, 44) = 2.217e-005, p = 0.9963; PFF treatment F (1, 44) = 0.01661, p = 0.8980; interaction F (1, 44) = 0.08812, p = 0.7680; Additional file 4: Figure S2d) or rotarod test (2-way ANOVA: genotype F (1, 45) = 0.08034, p = 0.7781; PFF treatment F (1, 45) = 2.507, p = 0.1203; interaction F (1, 45) = 0.02684, p = 0.8706; Additional file 4: Figure S2e).

We did observe a strong effect of PFF injections in WT animals in the social dominance test, which is thought to be a measure of prefrontal cortical and amygdala function [27, 30–33], at 6 mpi (Fig. 1c). PFF-injected transgenic 14-3-3 θ mice with 14-3-3 θ overexpression primarily in

the cortex showed a rescue of the social dominance deficit observed in WT littermates injected with PFFs (1-way ANOVA: F (2, 59) = 5.581; p = 0.0060; Fig. 1c).

Since our transgenic 14-3-3 θ line does not demonstrate 14-3-3 θ overexpression in the nigra (Additional file 2: Figure S3b), we tested the impact of 14-3-3 θ overexpression in the SN using an adeno-associated virus (AAV) expressing 14-3-3 θ -GFP [18]. WT mice were stereotactically injected with AAV-GFP or AAV-14-3-3 θ /GFP into the SN at 8 weeks of age, and then monomeric or fibrillar α syn was injected into the ipsilateral dorsolateral striatum four weeks later. While there was a slight PFF effect on the open field test (2 way ANOVA: genotype F (1, 52) = 0.04865, p = 0.8263; PFF treatment F (1, 52) = 10.01, p = 0.0026, interaction (1, 52) = 0.2352, p = 0.6297) and on the pole test (2 way ANOVA: genotype F (1, 52) = 0.02336, p = 0.8791; PFF treatment F (1, 52) = 4.251, p = 0.0442; interaction F (1, 52) = 0.7770, p = 0.3821), no significant differences were observed between GFP mice injected with monomer vs. GFP mice injected with PFFs or between GFP mice injected with PFFs and 14-3-3 θ mice injected with PFFs on either pole test or open field testing at 6 mpi (Additional file 4: Figure S2i–k). No significant motor deficit was observed in mice injected with AAV-GFP or AAV-14-3-3 θ /GFP with or without PFFs in the wire hang test at 6 mpi (2-way ANOVA: genotype F (1, 52) = 1.554, p = 0.2181; PFF treatment F (1, 52) = 2.342, p = 0.1320; interaction F (1, 52) = 0.2655, p = 0.6086; Additional file 4: Figure S2l).

14-3-3 inhibition exacerbates social dominance behavioral deficits induced by α syn fibrils

We next examined whether inhibition of 14-3-3s with the pan-14-3-3 peptide inhibitor difopein affects behavioral deficits in the in vivo PFF model. Transgenic mice expressing difopein in the cortex showed a deficit in social dominance after PFF injection that was not observed in WT mice at 3 mpi (1-way ANOVA: F (2, 42) = 3.139, p = 0.05; Fig. 1d). At 6 mpi, the win rate on the social dominance test was lower in difopein mice injected with PFFs compared to WT mice injected with PFFs (1-way ANOVA: F (2, 41) = 7.359, p = 0.0019; Fig. 1e). PFF treatment showed an overall slight increase in velocity (2-way ANOVA: genotype F (1, 56) = 0.4789, p = 0.4918; PFF effect F (1, 56) = 10.57, p = 0.0020; interaction F (1, 56) = 0.2741, p = 0.6027) and distance traveled (2-way ANOVA: genotype F (1, 56) = 0.1289, p = 0.7209; PFF effect F (1, 56) = 11.94, p = 0.0011; interaction F (1, 56) = 0.6675, p = 0.4174) in mice on the open field test, but no dramatic differences were noted between individual experimental groups at 6 mpi (Additional file 4: Figure S2f, g). No differences were noted between genotype or PFF treatment in the percent time

spent in the periphery of the open field arena (2-way ANOVA: genotype $F(1, 56) = 0.3703$, $p = 0.5453$; PFF treatment $F(1, 56) = 0.6636$; $p = 0.4187$; interaction $F(1, 56) = 0.9522$, $p = 0.3333$; Additional file 4: Figure S2h).

Similar to that observed with the AAV-14-3-3 θ injections into the SN, expression of difopein in the SN did not impact motor function significantly. PFF or genotype did not impact distance traveled (2-way ANOVA: genotype effect $F(1, 60) = 0.6861$, $p = 0.4108$; PFF treatment $F(1, 60) = 0.2927$, $p = 0.5905$; interaction $F(1, 60) = 5.109$; $p = 0.0274$) or velocity (2-way ANOVA: genotype effect $F(1, 60) = 0.2982$, $p = 0.5870$; PFF treatment $F(1, 60) = 0.03472$, $p = 0.8528$; interaction $F(1, 60) = 13.13$, $p = 0.0006$) on the open field test at 6 mpi, although a slight interaction effect was noted (Additional file 4: Figure S2m, n). WT and nigral difopein mice did not demonstrate any motor deficit on the rotarod test at 6 mpi (2-way ANOVA: genotype $F(1, 56) = 0.6888$, $p = 0.4101$; PFF treatment $F(1, 56) = 2.386$, $p = 0.1281$; interaction $F(1, 56) = 0.09658$, $p = 0.7571$; Additional file 4: Figure S2o, p).

14-3-3 θ overexpression delays α syn inclusion formation

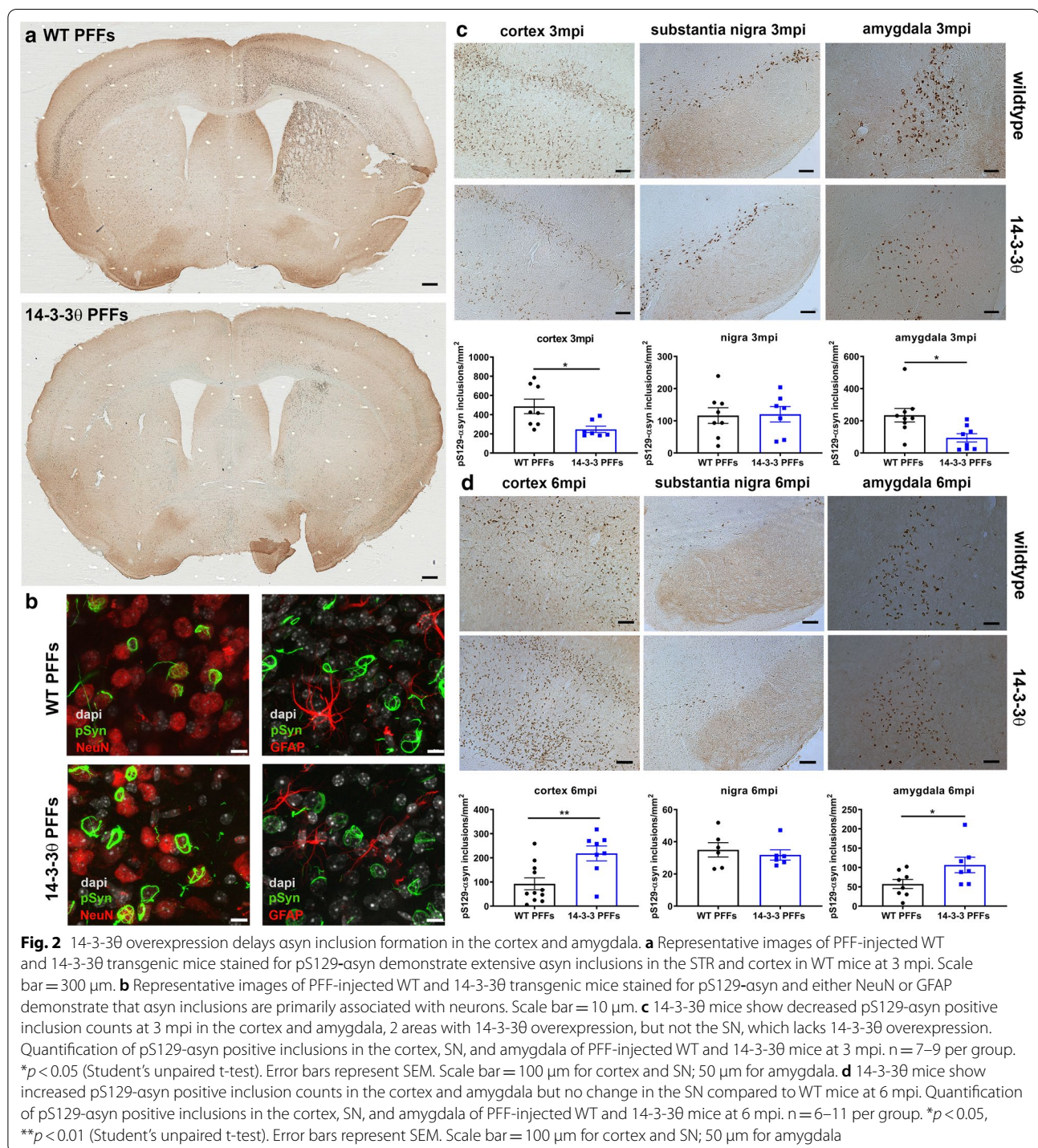
Given the reversal of the social dominance deficit in 14-3-3 θ mice, we next examined the impact of 14-3-3 θ on α syn inclusion formation. At 3 mpi, we observed a dramatic number of inclusions that stained positive for phosphorylated S129- α syn (pS129- α syn) in the sensorimotor cortex of WT mice injected with PFFs (Fig. 2a, c). By 6 mpi, inclusion numbers in WT mice were dramatically reduced (Fig. 2d). Other groups have also noticed a decline in α syn inclusions over time in mice, presumably due to the loss of neurons that develop inclusions [34–36]. Monomer-injected mice failed to stain for pS129- α syn (Additional file 2: Figure S3a). Inclusions in PFF-injected mice were primarily associated with neurons instead of glial cells, as demonstrated by co-staining for pS129- α syn with the neuronal marker NeuN or the astrocytic marker GFAP (Fig. 2b; Additional file 2: Figure S3c). In 14-3-3 θ transgenic mice injected with PFFs compared to WT mice injected with PFFs, we observed a 41% reduction in the number of inclusions that stained positive for pS129- α syn in the cortex at 3 mpi (unpaired, two-tailed t-test: $t_{(13)} = 2.754$, $p = 0.0164$; Fig. 2a, c). However, at 6 mpi, 14-3-3 θ mice injected with PFFs showed a 2.4-fold increase in inclusion counts in the cortex compared to WT mice injected with PFFs (unpaired, two-tailed t-test: $t_{(17)} = 3.232$, $p = 0.0049$; Fig. 2d). These inclusions in 14-3-3 θ mice were also associated with neurons instead of glial cells (Fig. 2b; Additional file 2: Figure S3c). In the amygdala, we observed a 60% decrease in the number of pS129- α syn positive inclusions at 3 mpi in 14-3-3 θ transgenic mice injected with PFFs compared

to WT mice injected with PFFs (unpaired, two-tailed t-test: $t_{(15)} = 2.757$, $p = 0.0147$) but then a 60% increase in the number of inclusions in the amygdala at 6 mpi (unpaired, two-tailed t-test: $t_{(13)} = 2.193$, $p = 0.0471$) in 14-3-3 θ transgenic mice injected with PFFs compared to WT mice injected with PFFs (Fig. 2c, d). No differences in inclusion counts were noted between 14-3-3 θ and WT mice at either 3 mpi (unpaired, two-tailed t-test: $t_{(13)} = 0.1161$, $p = 0.9094$) or 6 mpi (unpaired, two-tailed t-test: $t_{(10)} = 0.5746$, $p = 0.5782$) in the SN, in which 14-3-3 θ overexpression is not seen in these transgenic mice (Fig. 2c, d). These findings suggest that inclusion formation in the cortex and amygdala is delayed by 14-3-3 θ overexpression, and that higher levels of inclusions seen at 6 mpi in the 14-3-3 θ mice compared to WT mice could be due to a reduction in neuronal loss.

Since our transgenic 14-3-3 θ line does not demonstrate 14-3-3 θ overexpression in the SN, we also examined nigral inclusion formation in the mice stereotactically injected with AAV-GFP or AAV-14-3-3 θ /GFP in the SN (Fig. 3a). Consistent with our transgenic data, the number of inclusions positive for pS129- α syn in the SN was decreased in mice injected with AAV-14-3-3 θ /GFP compared to mice injected with AAV-GFP at 3 mpi (unpaired, two-tailed t-test: $t_{(25)} = 2.229$, $p = 0.0350$ Fig. 3b, d). By 6 mpi, the number of inclusions positive for pS129- α syn in the SN were increased in mice injected with AAV-14-3-3 θ /GFP compared to mice injected with AAV-GFP (unpaired, two-tailed t-test: $t_{(25)} = 2.481$, $p = 0.0202$; Fig. 3c, d). As observed in the 14-3-3 θ transgenic mice, the pS129- α syn inclusions were associated primarily with neurons instead of glial cells (Fig. 3e). These findings suggest that inclusion formation in the nigra is also delayed by 14-3-3 θ overexpression in the SN. The subsequent increase in inclusion formation at 6 mpi could reflect a reduction in neuronal loss in mice overexpressing 14-3-3 θ in the SN.

14-3-3 inhibition accelerates α syn inclusion formation

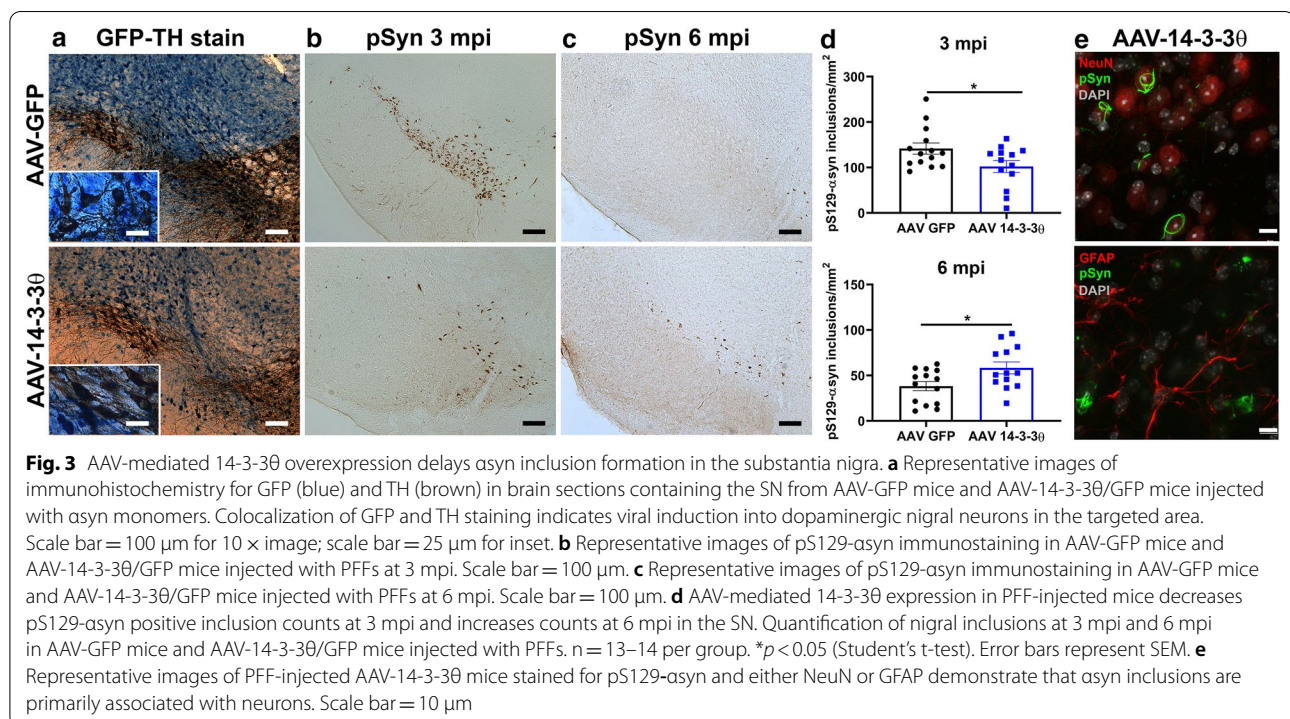
We next examined whether inhibition of 14-3-3s with the pan-14-3-3 peptide inhibitor difopein affects α syn inclusion formation in the in vivo PFF model. The difopein transgenic line that expresses difopein-eYFP in neurons in the cortex but not within the SN revealed increased inclusion counts in the cortex at 3 mpi compared to WT mice (unpaired, two-tailed t-test: $t_{(29)} = 2.441$, $p = 0.0210$; Fig. 4a–c). However, at 6 mpi, inclusion counts were significantly lower by 43% in the cortical difopein mice compared to WT injected with PFFs (unpaired, two-tailed t-test: $t_{(25)} = 2.233$, $p = 0.0347$; Fig. 4c). Similarly, in the amygdala, inclusion counts were increased by 31% at 3 mpi (unpaired, two-tailed t-test: $t_{(21)} = 2.070$, $p = 0.05$) but showed a non-significant decrease (53%) at 6 mpi



(unpaired, two-tailed t-test: $t_{(15)} = 2.021$, $p = 0.0616$) in difopein mice compared to WT mice (Additional file 3: Figure S4).

To test the impact of 14-3-3 inhibition on aggregation in nigral neurons, we measured inclusions in the nigral difopein transgenic line. Inclusion counts in the difopein

nigral mice showed a non-significant increase at 3 mpi (unpaired, two-tailed t-test: $t_{(14)} = 1.123$, $p = 0.2804$) and decreased significantly at 6 mpi (unpaired, two-tailed t-test: $t_{(21)} = 2.355$, $p = 0.0283$) after PFF injection compared to WT mice (Fig. 4d-f). We conclude that 14-3-3 inhibition accelerates inclusion formation in response to



α syn fibrils, and that the reduction in inclusion counts at 6 mpi could reflect an increase in neuronal loss.

14-3-3s regulate reduction in dopaminergic neuron counts induced by α syn fibrils

As noted above, α syn inclusion numbers are much higher at 3 months after PFF injection than at 6 months after injection in WT animals. This reduction in α syn inclusion numbers over time is presumably secondary to the death of neurons that develop α syn inclusions [35]. 14-3-3 θ overexpression in either the nigra or cortex reduced α syn inclusion numbers at 3 mpi, but we observed an increase in α syn inclusions at 6 mpi in 14-3-3 θ -overexpressing mice compared to control mice. We hypothesized that this delayed increase in inclusion formation with 14-3-3 θ overexpression is due to the rescue of neurons that normally die in response to PFFs in control mice. To test the impact of 14-3-3 θ overexpression on dopaminergic neurons in the SN, we performed stereological analysis of TH-positive neuronal counts in the nigra in mice injected with AAV-GFP or AAV-14-3-3 θ /GFP. As expected, striatal PFFs induced a 25% reduction in ipsilateral dopaminergic neuron counts in control mice injected with AAV-GFP into the ipsilateral nigra at 6 mpi (2-way ANOVA: genotype $F(1, 43) = 0.8197$, $p = 0.3703$; PFF treatment $F(1, 43) = 10.01$, $p = 0.0029$; interaction $F(1, 43) = 2.514$, $p = 0.1202$; Fig. 5a, b). In contrast, AAV-14-3-3 θ /GFP

mice injected with PFFs did not demonstrate a significant reduction in TH-positive dopaminergic neurons compared to AAV-14-3-3 θ /GFP mice injected with monomeric α syn at 6 mpi (Fig. 5a, b). This finding suggests that the increase in α syn inclusions in 14-3-3 θ -overexpressing mice at 6 mpi may be due to a reduction in dopaminergic neuronal loss.

We next examined TH-positive neuronal counts in response to PFFs in difopein-expressing mice. Stereological analysis of TH-positive counts in the nigra revealed a greater reduction in ipsilateral dopaminergic neuronal counts in PFF-injected mice expressing difopein in the SN compared to WT mice after PFF injection at 6 mpi (2-way ANOVA: genotype $F(1, 46) = 3.208$, $p = 0.0798$; PFF treatment $F(1, 46) = 58.27$, $p < 0.0001$; interaction $F(1, 46) = 4.309$, $p = 0.0435$; Fig. 5c, e). Stereological analysis at 3 mpi showed a non-significant reduction of TH-positive dopaminergic neuron numbers in difopein nigral mice, but no reduction in TH-positive dopaminergic neurons in WT mice injected with PFFs at 3 mpi (2-way ANOVA: genotype $F(1, 26) = 3.282$, $p = 0.0816$; PFF treatment $F(1, 26) = 0.3335$, $p = 0.5686$; interaction $F(1, 26) = 1.105$, $p = 0.3028$; Fig. 5d), as previously described by others [24]. We also examined whether TH-positive cell numbers correlated with pS129- α syn inclusion numbers, but the association varied between the different cohorts, with the only significant correlation in the difopein 6 mpi cohort (Additional file 5: Figure S5).

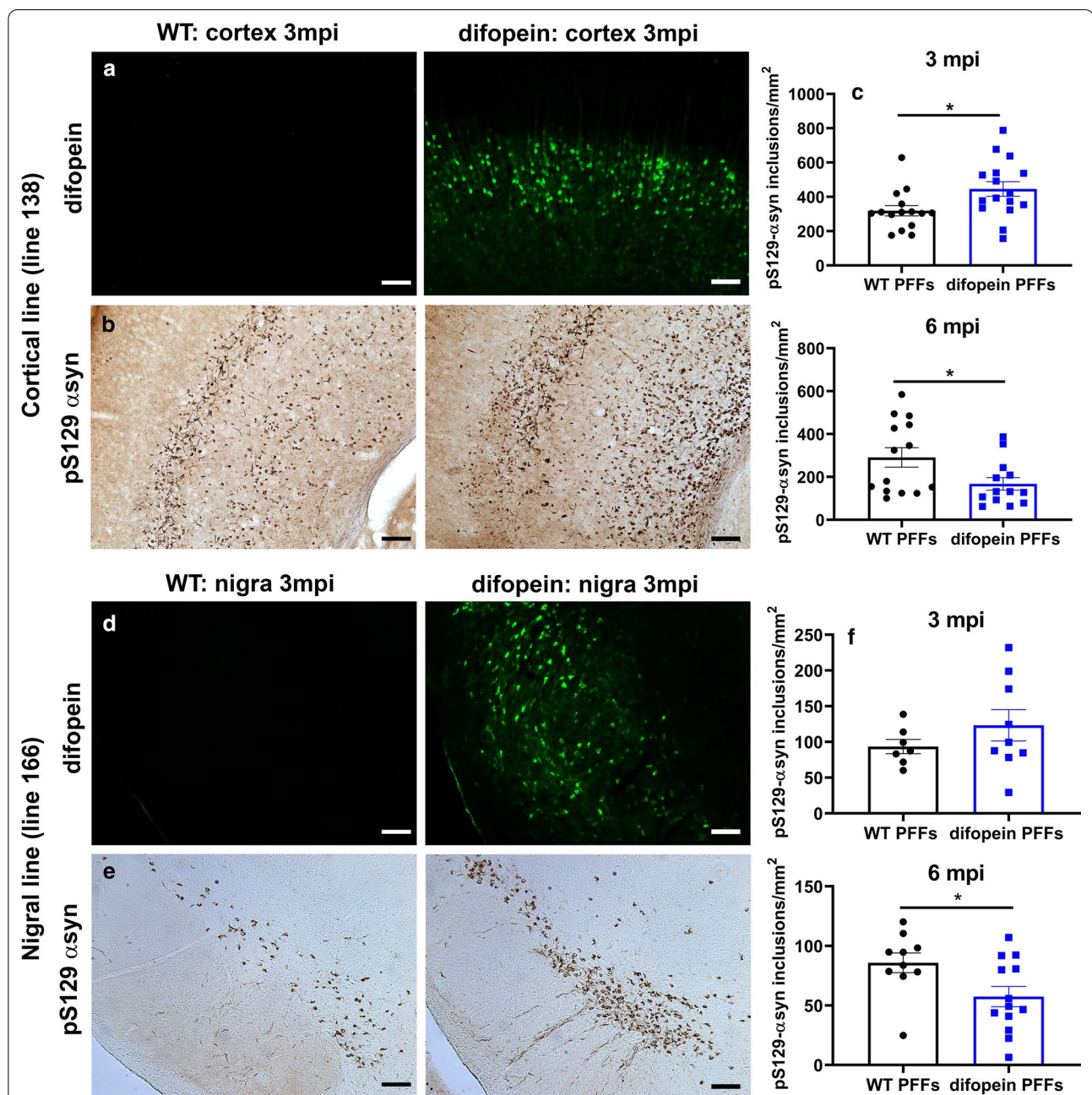
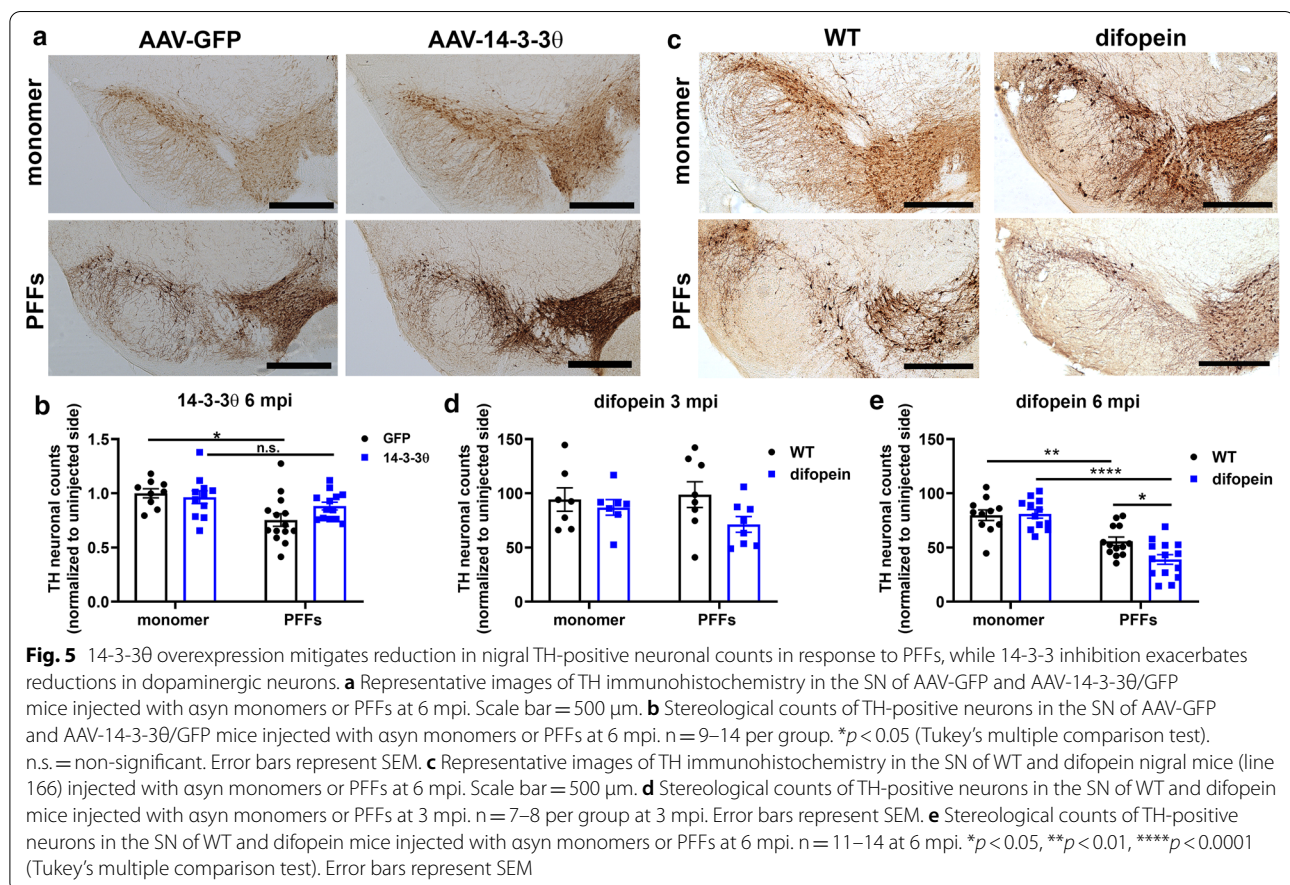


Fig. 4 14-3-3 inhibition increases asyn inclusion formation. **a** Representative images of eYFP-difopein immunostaining in the cortex of WT and difopein ("cortical" line 138) mice at 3 mpi. GFP-difopein expression is found only in difopein mice. Scale bar = 100 μm. **b** Representative images of pS129-α-syn immunostaining in the cortex of WT and difopein mice at 3 mpi. Scale bar = 100 μm. **c** Difopein expression in the cortex increases inclusion counts at 3 mpi and decreases counts at 6 mpi in the cortex. Quantification of pS129-α-syn positive inclusions at 3 mpi and 6 mpi in the cortex of PFF-injected WT or difopein mice. n = 15–16 per group at 3 mpi; n = 13–14 per group at 6 mpi. **p* < 0.05 (Student's *t*-test). Error bars represent SEM. **d** Representative images of eYFP-difopein immunostaining in the SN of WT and difopein ("nigral" line 166) mice at 3 mpi. GFP-difopein expression is found only in difopein mice. Scale bar = 100 μm. **e** Representative images of pS129-α-syn immunostaining in the SN of WT and difopein mice at 3 mpi. Scale bar = 100 μm. **f** Difopein expression in the nigra increases inclusion counts at 3 mpi and decreases counts at 6 mpi in the SN. Quantification of pS129-α-syn positive inclusions at 3 mpi and 6 mpi in the SN of PFF-injected WT and difopein mice. n = 7–9 per group at 3 mpi; n = 10–13 per group at 6 mpi. **p* < 0.05 (Student's *t*-test). Error bars represent SEM



To assess potential neuronal loss in the cortex of WT and transgenic difopein mice, we measured counts of layer IV pyramidal neurons. Since inclusion formation primarily occurs in layer IV and V pyramidal neurons [28], we used NECAB1 as a marker for layer IV pyramidal neurons and measured counts of NECAB1-positive neurons per area (Additional file 6: Figure S6b). At 6 mpi, we observed a non-significant reduction in NECAB1-positive neuronal density in WT mice injected with PFFs compared to those injected with monomeric asyn, while difopein mice injected with PFFs did show a significant reduction in NECAB1-positive neuronal density compared to difopein mice injected with monomeric asyn (2-way ANOVA: genotype $F(1, 27) = 1.426$, $p = 0.2428$; PFF treatment $F(1, 27) = 35.68$, $p < 0.0001$; interaction $F(1, 27) = 4.681$, $p = 0.0395$; Additional file 6: Figure S6a, c). While not statistically significant, there was a slight trend towards decreased NECAB1 counts in difopein mice injected with PFFs compared to WT mice injected with PFFs (Additional file 6: Figure S6a, c). These findings in the SN and cortex suggest that the reduction in asyn inclusion counts in difopein-expressing mice at 6

mpi could be due to the increased loss of neurons in difopein mice compared to WT mice.

Discussion

In this study we examined the role of 14-3-3s on asyn aggregation and neuronal toxicity in the *in vivo* preformed fibril (PFF) mouse model. We tested the effects of 14-3-3 θ overexpression and 14-3-3 inhibition by the pan-peptide inhibitor difopein in either the cortex or the SN at 2 time points after PFF injection. 14-3-3 θ overexpression in the cortex and amygdala, as demonstrated in our 14-3-3 θ transgenic line, delayed asyn inclusion formation and rescued the social dominance deficit. 14-3-3 θ overexpression in the SN by AAV also delayed asyn inclusion formation and partially rescued reductions in TH-positive neuronal counts. In contrast, difopein expression accelerated asyn inclusion formation, the social dominance behavioral deficit, and reductions in TH-positive and NECAB1-positive neuronal counts. These results suggest that 14-3-3s act as a chaperone to reduce asyn aggregation and its resulting toxicity on behavioral function and neuronal populations.

We and other groups have demonstrated that inclusion formation in the mouse PFF model peaks around 3 months after PFF injection with a subsequent reduction in inclusions at later time points [24, 34]. This reduction in aggregates coincides with the onset of TH-positive neuronal count reduction at 6 mpi [24, 34], suggesting that the reduction in aggregate numbers is due to the death of neurons with inclusions. Indeed, live imaging has demonstrated that neurons displaying α syn inclusions ultimately die when tracked over time [35]. In our study, we found that 14-3-3 θ overexpression decreased α syn aggregation at 3 mpi, but interestingly increased α syn aggregate counts at 6 mpi in areas expressing higher levels of 14-3-3 θ . Conversely, 14-3-3 inhibition increased α syn aggregation at 3 mpi but decreased it at 6 mpi in areas expressing difopein. We hypothesize that the subsequent increase in inclusion numbers with 14-3-3 θ overexpression at 6 mpi is due to a delay in neuronal loss as compared to that seen in WT mice. Conversely, the decrease in inclusion numbers in difopein mice at 6 mpi is likely secondary to an acceleration of cell death relative to WT mice. Indeed, our analyses of neuronal counts and behavior are consistent with this interpretation. 14-3-3 θ overexpression limited reductions in dopaminergic TH-positive neuron counts in the SN at 6 mpi, and behavioral rescue also points to rescue of neuronal function. Conversely, 14-3-3 inhibition promoted a greater reduction in TH-positive dopaminergic neuronal cell counts at 6 mpi. Although not significant, 14-3-3 inhibition trended towards reduced dopaminergic cell counts at 3 mpi as well, suggesting an acceleration of dopaminergic cell death. We did see a significant correlation between TH-positive neuronal counts and inclusion numbers in the difopein 6 mpi cohort, but otherwise differences in TH-positive stereological neuronal counts did not consistently correlate with inclusion counts. This could be due to variability between neurons and/or between mice with regard to when aggregates first form and when neurons die. Of note, decreases in TH-positive cell counts may be due to decreased expression of TH in dopaminergic neurons, which may indicate a functional deficit instead of overt neuronal cell loss. However, our results are consistent with others demonstrating neuronal cell loss in the SN at 6 mpi [37]. Additionally, NECAB1-positive cell counts in the sensorimotor cortex were also reduced in PFF-injected difopein mice, further suggesting that neuronal cell loss is occurring in multiple brain regions. The acceleration of the social dominance defect in difopein mice is consistent with this acceleration of cortical neuron loss.

pS129- α syn positive inclusions were predominantly localized in neurons, suggesting a neuronal selective vulnerability in this model. Previous groups have established

that genetic α syn mouse models with or without PFF treatment can demonstrate the formation of inclusions in glial populations, such as astrocytes, particularly at late stages [38–42]. Few to no inclusions colocalized with the astrocytic marker GFAP at 6 mpi, suggesting that 14-3-3 θ 's effects on inclusion numbers primarily involve neurons, although we cannot fully rule out the possibility that 14-3-3 θ 's increase in inclusion numbers at 6 mpi could also reflect some inclusion formation within glial cells. Additionally, 14-3-3 θ transgenic expression is driven under the Thy1 neuronal promoter, further suggesting that differences in inclusion load primarily occur in neurons.

In order to assess the effects of 14-3-3s on α syn toxicity in the PFF model, we used both transgenic and AAV-induced expression mouse models. Reproducible and consistent findings between AAV and transgene methods of 14-3-3 θ overexpression suggest that our findings are not an artifact of transgene expression. The use of both methods also allowed for the assessment of selective areas of expression in modulating the effects of α syn after initial aggregation initiated by PFF injection in the striatum, as α syn inclusion formation is seen throughout multiple brain regions in both PD patients and in the PFF model. Our findings demonstrate that 14-3-3s' effects on α syn are not restricted to particular brain regions, but that 14-3-3s can impact α syn pathology in multiple areas in which α syn pathology is observed in the PFF model. Of note, we tested the effects of the overexpression of a single isoform 14-3-3 θ in comparison to pan inhibition of 14-3-3 isoforms by difopein. Our lab has previously established the integral role of 14-3-3 θ in modulating α syn spread and toxicity [4], although other isoforms may also impact α syn pathology. For example, 14-3-3 η can regulate α syn aggregation in vitro [43]. We used the pan-14-3-3 peptide inhibitor to eliminate the possibility that other 14-3-3 isoforms could compensate for lack of a single isoform.

14-3-3 proteins interact with multiple aggregation-prone proteins in neurodegenerative diseases, including tau, huntingtin, and α syn [44–49]. Our lab previously established that 14-3-3 θ acts as a chaperone to regulate α syn seeding, cell-to-cell transmission, and toxicity in both the paracrine α syn and in vitro PFF models [4]. 14-3-3 θ complexes with α syn to prevent its adoption of a pathologic conformation, limiting further α syn aggregation. 14-3-3 θ -complexed α syn decreases its uptake, seeding potential, and paracrine toxicity. Here we further confirm the essential role for 14-3-3 θ in the in vivo PFF model and predict that its protective effects in vivo involve its role as a chaperone. 14-3-3s could also act as a chaperone to regulate other aggregation-prone proteins, yet whether 14-3-3s do regulate other aggregation-prone

proteins in vivo is yet to be determined. In vitro studies evaluating the impact of 14-3-3s on tau and huntingtin aggregation have been mixed [50–55].

Based on our findings here and in other studies, we propose that disruption of 14-3-3 function may serve to promote the neurodegenerative process in PD and DLB. Alterations in 14-3-3s have been noted in PD models and in human disease [14–17, 56]. We have previously shown that increased α syn levels reduces 14-3-3 θ expression in α syn cellular and mouse models and that 14-3-3 levels are reduced in DLB [14–17]. Additionally, we have observed increased 14-3-3 θ phosphorylation in PD models and in human PD and DLB brains [15, 56]. A reduction in 14-3-3 levels and aberrant 14-3-3 phosphorylation may impair the chaperone function of 14-3-3 θ to minimize α syn misfolding. Future studies are in progress to examine the impact of 14-3-3 phosphorylation on α syn pathology.

Motor phenotypes in the PFF model have been variably reported, with some groups finding strong motor deficits and others observing none [24, 28, 29]. Our data showed no consistent deficits in PFF-injected mice by wire hang, pole test, or rotarod at 6 mpi. Variability in behavioral deficits may be due to differences in protocol or in the genetic background of the mice used in each study. This lack of replication may also be due to differences in the synthesis of injected fibrils, resulting in different rates of α syn aggregation and neuronal cell death. It has been previously established that α syn aggregates reach different peak times in each brain region and then decrease as the aggregates are cleared and cells die [24, 34–36]. As a result, behavioral phenotypes in this model may vary based on the seeding potential of the PFFs injected. Interestingly, we consistently observed deficits in the social dominance tube test in PFF-injected mice at 6 mpi, pointing to strong implications for prefrontal cortical and amygdala involvement in this model, reflecting a disease profile reminiscent of DLB [28].

Conclusion

In conclusion, we found that 14-3-3 θ overexpression reduced behavioral deficits, delayed α syn aggregation, and partially prevented decreases in TH-positive neuronal counts, while 14-3-3 inhibition accelerated behavioral deficits, α syn aggregation, and reductions in TH-positive neurons in the PFF mouse model. Our work here further demonstrates the neuroprotective effects of 14-3-3 θ overexpression in multiple brain regions, indicating that this protective mechanism applies broadly to multiple cell types affected by α syn pathology. Together these data indicate the role of 14-3-3s in the regulation of α syn pathology and their therapeutic potential as a molecular target for synucleinopathies. Induction of

14-3-3 θ may prove to be a viable technique for slowing disease progression.

Supplementary Information

The online version contains supplementary material available at <https://doi.org/10.1186/s40478-020-01110-5>.

Additional file 1: Figure S1 Verification of sonicated fibril radius by dynamic light scattering (DLS). (a) Representative DLS graph of average sonicated fibril radius shown for WT and 14-3-3 θ transgenic mice injected for the 6 mpi time point. After sonication, PFFs were confirmed by Nanodrop for concentration and analyzed by DLS to ensure a mean radius of 20–50 nm for sonicated fibrils. PFFs were reassessed by DLS at the beginning of each day of injections. (b) Representative TEM of α syn fibrils before sonication. Scale bar = 200 nm. (c) Representative TEM of α syn fibrils after sonication. Scale bar = 200 nm.

Additional file 2: Figure S2 Motor behaviors are not affected by PFF treatment nor by 14-3-3 manipulation in the cortex, amygdala, or nigra. (a–c) Quantification of average velocity (a), distance traveled (b), and percent time in the periphery (c) in the open field test for WT and 14-3-3 θ mice injected with α syn monomer or PFFs at 6 mpi. n = 11–14 per group, *p < 0.05 (Tukey's multiple comparison test) (Tukey's multiple comparison test). Error bars represent SEM. (d) Quantification of time to reach the bottom in the pole test for WT and 14-3-3 θ mice injected with α syn monomer or PFFs at 6 mpi. n = 11–14 per group, n.s. (Tukey's multiple comparison test). Error bars represent SEM. (e) Quantification of latency to fall in the accelerating rotarod test on the second assessment day after 3 days of training for WT and 14-3-3 θ mice injected with α syn monomer or PFFs at 6 mpi. n = 11–14 per group, n.s. (Tukey's multiple comparison test). Error bars represent SEM. (f, h) Quantification of average velocity (f), distance traveled (g), and time in periphery (h) in the open field test for WT and difopein ("cortical" line 138) mice injected with α syn monomer or PFFs at 6 mpi. n = 14–16 per group, *p < 0.05 (Tukey's multiple comparison test). Error bars represent SEM. (i–l) Quantification of average velocity (i) and distance traveled (j) in the open field test, time to reach the bottom in the pole test (k), and latency to fall on the wire hang test (l) in AAV-GFP and AAV-14-3-3 θ /GFP mice injected with α syn monomer or PFFs at 6 mpi. n = 12–16 per group, n.s. (Tukey's multiple comparison test). Error bars represent SEM. (m–p) Quantification of average velocity (m) and distance traveled (n) in the open field test and latency to fall in the accelerating rotarod test (o, p) in WT and difopein ("nigral" line 166) mice injected with α syn monomer or PFFs at 6 mpi. n = 15–17 per group, *p < 0.05 (Tukey's multiple comparison test). Error bars represent SEM.

Additional file 3: Figure S3 α syn aggregation occurs primarily in neurons at 6 months post injection. (a) Representative images of pS129- α syn immunostaining in the cortex at 6 mpi in WT and 14-3-3 θ mice injected with α syn monomer into the striatum. Scale bar = 100 μ m. (b) Representative images of HA immunostaining in the cortex, SN, and amygdala demonstrates that HA-tagged 14-3-3 θ is expressed in cortical and amygdala regions, but not in the SN. Scale bar = 100 μ m for cortex and SN; 50 μ m for amygdala. (c) pS129- α syn inclusions associate primarily with NeuN instead of GFAP in PFF-injected WT and 14-3-3 θ transgenic mice at 6 mpi. Scale bar = 50 μ m.

Additional file 4: Figure S4 α syn aggregation is accelerated in the amygdala in mice expressing difopein in the amygdala. (a) Representative images of eYFP-difopein immunostaining in the amygdala of WT and difopein ("cortical" line 138) mice at 3 mpi. GFP-difopein expression is found only in difopein mice. Scale bar = 100 μ m. (b) Representative images of pS129- α syn immunostaining in the cortex of WT and difopein mice at 3 and 6 mpi. Scale bar = 100 μ m. (c) Difopein expression increases inclusion counts in PFF-injected mice at 3 mpi. Quantification of pS129- α syn positive inclusions at 3 mpi and 6 mpi in the amygdala of PFF-injected WT and difopein mice. n = 11–12 per group at 3 mpi, n = 8–9 at 6 mpi. *p < 0.05 (Student's t-test). Error bars represent SEM.

Additional file 5: Figure S5 pS129- α syn positive inclusions do not consistently correlate with TH-positive neuronal cell counts. (a) pS129- α syn

positive inclusions and TH-positive cell counts in PFF-injected AAV-14-3-3 β /GFP and AAV-GFP mice at 6 mpi (Pearson $r = -0.00369$, $p = 0.9854$). (b) pS129- α syn positive inclusions and TH-positive cell counts in PFF-injected difopein and WT mice at 3 mpi (Pearson $r = -0.3814$, $p = 0.145$). (c) pS129- α syn positive inclusions and TH-positive cell counts in PFF-injected difopein and WT mice at 6 mpi (Pearson $r = 0.7157$, $p = 0.0001$).

Additional file 6: Figure S6 Difopein promotes the reduction of NECAB1-positive neurons in response to PFFs. (a) Representative images of NECAB1-positive immunostaining in the cortex of WT and difopein mice injected with α syn monomers or PFFs at 6 mpi. Scale bar = 100 μ m. (b) pS129- α syn (red) immunostaining is concentrated in NECAB1-positive (green) IV and V layers of the sensorimotor cortex in a PFF-injected WT mouse. Scale bar = 50 μ m. (c) PFF-injected difopein mice have decreased NECAB1 counts in comparison to monomer-injected difopein mice. Quantification of NECAB1-positive neurons in the cortex of WT and difopein mice injected with α syn monomers or PFFs at 6 mpi. $n = 7-8$ per group. **** $p < 0.0001$ (Tukey's multiple comparison test). Error bars represent SEM.

Abbreviations

AAV: Adenovirus associated virus; α syn: Alpha-synuclein; CTX: Cortex; DLB: Dementia with Lewy Bodies; GFAP: Glial fibrillary acidic protein; IHC: Immunohistochemistry; LB: Lewy body; mpi: Months post injection; PD: Parkinson's disease; PFF: Pre-formed fibrils; pS129: Phosphoserine 129; SN: Substantia nigra; TEM: Transmission electron microscopy; TH: Tyrosine hydroxylase.

Acknowledgements

We are grateful to Drs. Laura Volpicelli-Daley and Andrew West for provision of recombinant α syn. We thank Dr. Yi Zhou at Florida State University who provided the difopein mouse lines that were used in these studies. Research reported in this publication was also supported by the UAB High Resolution Imaging Facility.

Authors' contributions

RU designed and performed experiments, analyzed data, and wrote manuscript. MG designed and performed experiments, analyzed data, and reviewed manuscript. NK, AK, SC, and AP performed experiments and reviewed manuscript. TY designed experiments, analyzed data, and wrote and finalized manuscript. All authors read and approved the final manuscript.

Funding

This study was supported by NIH [R01 NS088533 (TAY); R01 NS112203 (TAY); P50 NS108675 (TAY); F31 NS106733 (RU)], American Parkinson Disease Association, and the Parkinson Association of Alabama. These funding agencies had no role in the design of the study and collection, analysis, and interpretation of data and in writing the manuscript.

Availability of data and materials

The datasets generated and analyzed during the current study are available from the corresponding author on reasonable request.

Ethics approval and consent to participate

Mice were used in accordance with the guidelines of the National Institute of Health (NIH) and University of Alabama at Birmingham (UAB) Institutional Animal Care and Use Committee (IACUC) and all experiments abided by the principles outlined in the Basel Declaration.

Consent for publication

Not applicable.

Competing interests

Dr. Yacoubian has a U.S. Patent No. 7,919,262 on the use of 14-3-3s in neurodegeneration. The remaining authors have no competing interests to declare.

Author details

¹ Department of Neurology, Center for Neurodegeneration and Experimental Therapeutics, University of Alabama at Birmingham, Birmingham, AL 35294, USA. ² Civitan International Research Center, Room 510A, 1719 Sixth Avenue

South, Birmingham, AL 35294, USA. ³ Center for Neurodegenerative Disease Research, Perelman School of Medicine at the University of Pennsylvania, Maloney Building, 3rd Floor, 3600 Spruce Street, Philadelphia, PA 19104-2676, USA. ⁴ Medical Scientist Training Program, Northwestern University Feinberg School of Medicine, Chicago, IL 60611, USA.

Received: 25 August 2020 Accepted: 19 December 2020

Published online: 07 January 2021

References

- Cabin DE, Shimazu K, Murphy D, Cole NB, Gottschalk W, McIlwain KL, Orrison B, Chen A, Ellis CE, Paylor R (2002) Synaptic vesicle depletion correlates with attenuated synaptic responses to prolonged repetitive stimulation in mice lacking α -synuclein. *J Neurosci* 22:8797–8807
- Emamzadeh FN (2016) Alpha-synuclein structure, functions, and interactions. *J Res Med Sci* 21:29–29. <https://doi.org/10.4103/1735-1995.181989>
- Nemani VM, Lu W, Berge V, Nakamura K, Onoa B, Lee MK, Chaudhry FA, Nicoll RA, Edwards RH (2010) Increased expression of α -synuclein reduces neurotransmitter release by inhibiting synaptic vesicle recluster after endocytosis. *Neuron* 65:66–79. <https://doi.org/10.1016/j.neuron.2009.12.023>
- Wang B, Underwood R, Kamath A, Britain C, McFerrin MB, McLean PJ, Volpicelli-Daley LA, Whitaker RH, Placzek WJ, Becker K et al (2018) 14-3-3 proteins reduce cell-to-cell transfer and propagation of pathogenic α -synuclein. *J Neurosci* 38:8211–8232. <https://doi.org/10.1523/jneurosci.1134-18.2018>
- Kajiwara Y, Buxbaum JD, Grice DE (2009) SLITRK1 binds 14-3-3 and regulates neurite outgrowth in a phosphorylation-dependent manner. *Biol Psychiatry* 66:918–925
- Lavalley NJ, Slone SR, Ding H, West AB, Yacoubian TA (2016) 14-3-3 Proteins regulate mutant LRRK2 kinase activity and neurite shortening. *Hum Mol Genet* 25:109–122
- Mrowiec T, Schwappach B (2006) 14-3-3 proteins in membrane protein transport. *Biol Chem* 387:1227–1236
- Ramsler EM, Buck F, Schachner M, Tilling T (2010) Binding of all spectrin to 14-3-3 β is involved in NCAM-dependent neurite outgrowth. *Mol Cell Neurosci* 45:66–74
- Shandala T, Woodcock JM, Ng Y, Biggs L, Skoulakis EM, Brooks DA, Lopez AF (2011) Drosophila 14-3-3 ϵ has a crucial role in anti-microbial peptide secretion and innate immunity. *J Cell Sci* 124:2165–2174
- Vincenz C, Dixit VM (1996) 14-3-3 proteins associate with A20 in an isoform-specific manner and function both as chaperone and adapter molecules. *J Biol Chem* 271:20029–20034
- Yano M, Nakamura S, Wu X, Okumura Y, Kido H (2006) A novel function of 14-3-3 protein: 14-3-3 ζ is a heat-shock-related molecular chaperone that dissolves thermal-aggregated proteins. *Mol Biol Cell* 17:4769–4779
- Berg D, Riess O, Bornemann A (2003) Specification of 14-3-3 proteins in Lewy bodies. *Ann Neurol* 54:135–135
- Kawamoto Y, Akiguchi I, Nakamura S, Honjyo Y, Shibusaki H, Budka H (2002) 14-3-3 proteins in Lewy bodies in parkinson disease and diffuse Lewy body disease brains. *J Neuropathol Exp Neurol* 61:245–253. <https://doi.org/10.1093/jnen/61.3.245>
- Ding H, Fineberg NS, Gray M, Yacoubian TA (2013) α -Synuclein overexpression represses 14-3-3 θ transcription. *J Mol Neurosci* 51:1000–1009. <https://doi.org/10.1007/s12031-013-0086-5>
- McFerrin MB, Chi X, Cutter G, Yacoubian TA (2017) Dysregulation of 14-3-3 proteins in neurodegenerative diseases with Lewy body or Alzheimer pathology. *Ann Clin Transl Neurol* 4:466–477. <https://doi.org/10.1002/acn3.421>
- Yacoubian TA, Cantuti-Castelvetri I, Bouzou B, Asteris G, McLean PJ, Hyman BT, Standaert DG (2008) Transcriptional dysregulation in a transgenic model of Parkinson disease. *Neurobiol Dis* 29:515–528
- Yacoubian TA, Slone SR, Harrington AJ, Hamamichi S, Schieltz JM, Caldwell KA, Caldwell GA, Standaert DG (2010) Differential neuroprotective effects of 14-3-3 proteins in models of Parkinson's disease. *Cell Death Dis* 1:e2–e2
- Ding H, Underwood R, Lavalley N, Yacoubian TA (2015) 14-3-3 inhibition promotes dopaminergic neuron loss and 14-3-3 θ overexpression

- promotes recovery in the MPTP mouse model of Parkinson's disease. *Neuroscience* 307:73–82
19. Slone SR, Lesort M, Yacoubian TA (2011) 14-3-3 θ protects against neurotoxicity in a cellular Parkinson's disease model through inhibition of the apoptotic factor Bax. *PLoS ONE* 6:e21720
 20. Qiao H, Foote M, Graham K, Wu Y, Zhou Y (2014) 14-3-3 proteins are required for hippocampal long-term potentiation and associative learning and memory. *J Neurosci* 34:4801–4808. <https://doi.org/10.1523/jneurosci.4393-13.2014>
 21. Giasson BI, Murray IV, Trojanowski JQ, Lee VM-Y (2001) A hydrophobic stretch of 12 amino acid residues in the middle of α -synuclein is essential for filament assembly. *J Biol Chem* 276:2380–2386
 22. Volpicelli-Daley LA, Luk KC, Lee VM (2014) Addition of exogenous α -synuclein preformed fibrils to primary neuronal cultures to seed recruitment of endogenous α -synuclein to Lewy body and Lewy neurite-like aggregates. *Nat Protoc* 9:2135–2146. <https://doi.org/10.1038/nprot.2014.143>
 23. St Martin JL, Klucken J, Outeiro TF, Nguyen P, Keller-McGandy C, Cantuti-Castelvetri I, Grammatopoulos TN, Standaert DG, Hyman BT, McLean PJ (2007) Dopaminergic neuron loss and up-regulation of chaperone protein mRNA induced by targeted over-expression of alpha-synuclein in mouse substantia nigra. *J Neurochem* 100:1449–1457
 24. Luk KC, Kehm V, Carroll J, Zhang B, O'Brien P, Trojanowski JQ, Lee VM (2012) Pathological alpha-synuclein transmission initiates Parkinson-like neurodegeneration in nontransgenic mice. *Science* 338:949–953. <https://doi.org/10.1126/science.1227157>
 25. Steidinger TU, Slone SR, Ding H, Standaert DG, Yacoubian TA (2013) Angiogenesis in Parkinson disease models: role of Akt phosphorylation and evaluation of AAV-mediated angiogenesis expression in MPTP treated mice. *PLoS ONE* 8:e56092. <https://doi.org/10.1371/journal.pone.0056092>
 26. Klein SM, Vykoukal J, Lechler P, Zeitler K, Gehmert S, Schremel S, Alt E, Bogdahn U, Prantl L (2012) Noninvasive in vivo assessment of muscle impairment in the mdx mouse model—a comparison of two common wire hanging methods with two different results. *J Neurosci Methods* 203:292–297. <https://doi.org/10.1016/j.jneumeth.2011.10.001>
 27. Arrant AE, Filiano AJ, Warmus BA, Hall AM, Roberson ED (2016) Progranulin haploinsufficiency causes biphasic social dominance abnormalities in the tube test. *Genes Brain Behav* 15:588–603
 28. Stoyka LE, Arrant AE, Thrasher DR, Russell DL, Freire J, Mahoney CL, Narayanan A, Dib AG, Standaert DG, Volpicelli-Daley LA (2020) Behavioral defects associated with amygdala and cortical dysfunction in mice with seeded α -synuclein inclusions. *Neurobiol Dis* 134:104708
 29. Hayakawa H, Nakatani R, Ikenaka K, Aguirre C, Choong C-J, Tsuda H, Nagano S, Koike M, Ikeuchi T, Hasegawa M et al (2020) Structurally distinct α -synuclein fibrils induce robust parkinsonian pathology. *Mov Disord* 35:256–267. <https://doi.org/10.1002/mds.27887>
 30. Miczek KA, Brykczynski T, Grossman SP (1974) Differential effects of lesions in the amygdala, periamygdaloid cortex, and striatal terminalis on aggressive behaviors in rats. *J Comp Physiol Psychol* 87:760–771. <https://doi.org/10.1037/h0036971>
 31. Soumiya H, Godai A, Araiso H, Mori S, Furukawa S, Fukumitsu H (2016) Neonatal whisker trimming impairs fear/anxiety-related emotional systems of the amygdala and social behaviors in adult mice. *PLoS ONE* 11:e0158583–e0158583. <https://doi.org/10.1371/journal.pone.0158583>
 32. Wallén-Mackenzie Å, Nordenankar K, Fejgin K, Lagerström MC, Emilsson L, Fredriksson R, Wass C, Andersson D, Egecioglu E, Andersson M et al (2009) Restricted cortical and amygdaloid removal of vesicular glutamate transporter 2 in preadolescent mice impacts dopaminergic activity and neuronal circuitry of higher brain function. *J Neurosci* 29:2238–2251. <https://doi.org/10.1523/jneurosci.5851-08.2009>
 33. Zhou T, Sandi C, Hu H (2018) Advances in understanding neural mechanisms of social dominance. *Curr Opin Neurobiol* 49:99–107. <https://doi.org/10.1016/j.conb.2018.01.006>
 34. Abdelmotilib H, Maltbie T, Delic V, Liu Z, Hu X, Fraser KB, Moehle MS, Stoyka L, Anabtawi N, Krendelchtchikova V (2017) α -Synuclein fibril-induced inclusion spread in rats and mice correlates with dopaminergic neurodegeneration. *Neurobiol Dis* 105:84–98
 35. Osterberg Valerie R, Spinelli Kateri J, Weston Leah J, Luk Kelvin C, Woltjer Randall L, Unni Vivek K (2015) Progressive aggregation of alpha-synuclein and selective degeneration of Lewy inclusion-bearing neurons in a mouse model of parkinsonism. *Cell Rep* 10:1252–1260. <https://doi.org/10.1016/j.celrep.2015.01.060>
 36. Patterson JR, Duffy MF, Kemp CJ, Howe JW, Collier TJ, Stoll AC, Miller KM, Patel P, Levine N, Moore DJ et al (2019) Time course and magnitude of alpha-synuclein inclusion formation and nigrostriatal degeneration in the rat model of synucleinopathy triggered by intrastriatal α -synuclein preformed fibrils. *Neurobiol Dis* 130:104525. <https://doi.org/10.1016/j.nbd.2019.104525>
 37. Paumier KL, Luk KC, Manfredsson FP, Kanaan NM, Lipton JW, Collier TJ, Steece-Collier K, Kemp CJ, Celano S, Schulz E et al (2015) Intrastriatal injection of pre-formed mouse α -synuclein fibrils into rats triggers α -synuclein pathology and bilateral nigrostriatal degeneration. *Neurobiol Dis* 82:185–199. <https://doi.org/10.1016/j.nbd.2015.06.003>
 38. Mahul-Mellier A-L, Burtscher J, Maharjan N, Weerens L, Croisier M, Kuttler F, Leleu M, Knott GW, Lashuel HA (2020) The process of Lewy body formation, rather than simply α -synuclein fibrillization, is one of the major drivers of neurodegeneration. *Proc Natl Acad Sci* 117:4971–4982. <https://doi.org/10.1073/pnas.1913904117>
 39. Sacino AN, Brooks M, Thomas MA, McKinney AB, Lee S, Regenhardt RW, McGarvey NH, Ayers JJ, Notterpek L, Borchelt DR et al (2014) Intramuscular injection of α -synuclein induces CNS α -synuclein pathology and a rapid-onset motor phenotype in transgenic mice. *Proc Natl Acad Sci* 111:10732–10737. <https://doi.org/10.1073/pnas.1321785111>
 40. Schaser AJ, Stackhouse TL, Weston LJ, Kerstein J, Osterberg VR, López CS, Dickson DW, Luk KC, Meshul CK, Woltjer RL et al (2020) Trans-synaptic and retrograde axonal spread of Lewy pathology following pre-formed fibril injection in an in vivo A53T alpha-synuclein mouse model of synucleinopathy. *Acta Neuropathol Commun* 8:150. <https://doi.org/10.1186/s40478-020-01026-0>
 41. Sorrentino ZA, Brooks MMT, Hudson V, Rutherford NJ, Golde TE, Giasson BI, Chakrabarty P (2017) Intrastriatal injection of α -synuclein can lead to widespread synucleinopathy independent of neuroanatomic connectivity. *Mol Neurodegener* 12:40. <https://doi.org/10.1186/s13024-017-0182-z>
 42. Tanriöver G, Bacioglu M, Schweighauser M, Mahler J, Wegenast-Braun BM, Skodras A, Obermüller U, Barth M, Kronenberg-Versteeg D, Nilsson KPR et al (2020) Prominent microglial inclusions in transgenic mouse models of α -synucleinopathy that are distinct from neuronal lesions. *Acta Neuropathol Commun* 8:133. <https://doi.org/10.1186/s40478-020-00993-8>
 43. Plotegher N, Kumar D, Tessari I, Brucala M, Munari F, Tosatto L, Belluzzi E, Greggio E, Bisaglia M, Capaldi S et al (2014) The chaperone-like protein 14-3-3 η interacts with human α -synuclein aggregation intermediates rerouting the amyloidogenic pathway and reducing α -synuclein cellular toxicity. *Hum Mol Genet* 23:5615–5629. <https://doi.org/10.1093/hmg/ddu275>
 44. Foote M, Zhou Y (2012) 14-3-3 proteins in neurological disorders. *Int J Biochem Mol Biol* 3:152–164
 45. Hashiguchi M, Sobue K, Paudel HK (2000) 14-3-3 ζ is an effector of tau protein phosphorylation. *J Biol Chem* 275:25247–25254. <https://doi.org/10.1074/jbc.M003738200>
 46. Layfield R, Fergusson J, Aitken A, Lowe J, Landon M, Mayer RJ (1996) Neurofibrillary tangles of Alzheimer's disease brains contain 14-3-3 proteins. *Neurosci Lett* 209:57–60. [https://doi.org/10.1016/0304-3940\(96\)12598-2](https://doi.org/10.1016/0304-3940(96)12598-2)
 47. Shirasaki Dyna I, Greiner Erin R, Al-Ramahi I, Gray M, Boonthuep P, Geschwind Daniel H, Botas J, Coppola G, Horvath S, Loo Joseph A et al (2012) Network organization of the huntingtin proteomic interactome in mammalian brain. *Neuron* 75:41–57. <https://doi.org/10.1016/j.neuron.2012.05.024>
 48. Umahara T, Uchiyama T, Tsuchiya K, Nakamura A, Iwamoto T, Ikeda K, Takasaki M (2004) 14-3-3 proteins and zeta isoform containing neurofibrillary tangles in patients with Alzheimer's disease. *Acta Neuropathol* 108:279–286
 49. Waelter S, Boeddrich A, Lurz R, Scherzinger E, Lueder G, Lehrach H, Wanker EE (2001) Accumulation of mutant huntingtin fragments in aggresome-like inclusion bodies as a result of insufficient protein degradation. *Mol Biol Cell* 12:1393–1407
 50. Agarwal-Mawal A, Qureshi HY, Cafferty PW, Yuan Z, Han D, Lin R, Paudel HK (2003) 14-3-3 connects glycogen synthase kinase-3 β to tau within a brain microtubule-associated tau phosphorylation complex. *J Biol Chem* 278:12722–12728. <https://doi.org/10.1074/jbc.M211491200>

51. Omi K, Hachiya NS, Tanaka M, Tokunaga K, Kaneko K (2008) 14-3-3zeta is indispensable for aggregate formation of polyglutamine-expanded huntingtin protein. *Neurosci Lett* 431:45–50. <https://doi.org/10.1016/j.neulet.2007.11.018>
52. Papanikolopoulou K, Grammenoudi S, Samiotaki M, Skoulakis EM (2018) Differential effects of 14-3-3 dimers on tau phosphorylation, stability and toxicity in vivo. *Hum Mol Genet* 27:2244–2261
53. Qureshi HY, Li T, MacDonald R, Cho CM, Leclerc N, Paudel HK (2013) Interaction of 14-3-3 ζ with microtubule-associated protein tau within Alzheimer's disease neurofibrillary tangles. *Biochemistry* 52:6445–6455
54. Sadik G, Tanaka T, Kato K, Yamamori H, Nessa BN, Morihara T, Takeda M (2009) Phosphorylation of tau at Ser214 mediates its interaction with 14-3-3 protein: implications for the mechanism of tau aggregation. *J Neurochem* 108:33–43. <https://doi.org/10.1111/j.1471-4159.2008.05716.x>
55. Xu Z, Graham K, Foote M, Liang F, Rizkallah R, Hurt M, Wang Y, Wu Y, Zhou Y (2013) 14-3-3 protein targets misfolded chaperone-associated proteins to aggresomes. *J Cell Sci* 126:4173–4186. <https://doi.org/10.1242/jcs.126102>
56. Slone SR, Lavalley N, McFerrin M, Wang B, Yacoubian TA (2015) Increased 14-3-3 phosphorylation observed in Parkinson's disease reduces neuroprotective potential of 14-3-3 proteins. *Neurobiol Dis* 79:1–13. <https://doi.org/10.1016/j.nbd.2015.02.032>

Publisher's Note

Springer Nature remains neutral with regard to jurisdictional claims in published maps and institutional affiliations.

Ready to submit your research? Choose BMC and benefit from:

- fast, convenient online submission
- thorough peer review by experienced researchers in your field
- rapid publication on acceptance
- support for research data, including large and complex data types
- gold Open Access which fosters wider collaboration and increased citations
- maximum visibility for your research: over 100M website views per year

At BMC, research is always in progress.

Learn more biomedcentral.com/submissions

